Journal of Medicinal Chemistry

Article

pubs.acs.org/jmc

Tetraoxane–Pyrimidine Nitrile Hybrids as Dual Stage Antimalarials

Rudi Oliveira,[†] Rita C. Guedes,[†] Patrícia Meireles,[‡] Inês S. Albuquerque,[‡] Lídia M. Gonçalves,[†] Elisabete Pires,[§] Maria Rosário Bronze,[†,§] Jiri Gut,[∥] Philip J. Rosenthal,[∥] Miguel Prudêncio,[‡] Rui Moreira,*[,†] Paul M. O'Neill,*[,⊥] and Francisca Lopes[†]

[†]Instituto de Investigação do Medicamento (iMed.ULisboa), Faculdade de Farmácia, Universidade de Lisboa, Av. Prof. Gama Pinto, 1649-003 Lisboa, Portugal

[‡]Instituto de Medicina Molecular, Faculdade de Medicina da Universidade de Lisboa, Av. Prof. Egas Moniz, 1649-028 Lisboa, Portugal

[§]ITQB-UNL, Av. da República, Estação Agronómica Nacional, 2780-157 Oeiras, Portugal

[∥]Department of Medicine, San Francisco General Hospital, University of California, San Francisco, San Francisco, California 94143, United States

[⊥]Department of Chemistry, University of Liverpool, Liverpool, L69 3BX, U.K.

Supporting Information

ABSTRACT: The use of artemisinin or other endoperoxides in combination with other drugs is a strategy to prevent development of resistant strains of *Plasmodium* parasites. Our previous work demonstrated that hybrid compounds, comprising endoperoxides and vinyl sulfones, were capable of high activity profiles comparable to artemisinin and chloroquine while acting through two distinct mechanisms of action: oxidative stress and falcipain inhibition. In this study, we adapted this approach to a novel class of falcipain inhibitors: peptidomimetic pyrimidine nitriles. Pyrimidine tetraoxane hybrids displayed potent nanomolar activity against three strains of *Plasmodium falciparum* and falcipain-2, combined with low cytotoxicity. In vivo, a decrease in parasitemia and an increase in survival of mice infected with *Plasmodium berghei* was observed when compared to control. All tested compounds combined good blood stage activity with significant effects on liver stage parasitemia, a most welcome feature for any new class of antimalarial drug.

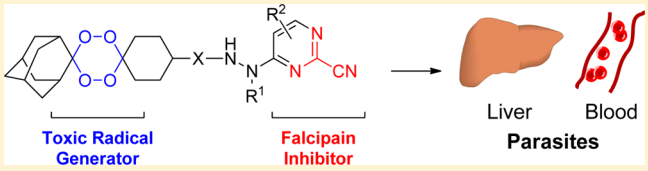

INTRODUCTION

Although the number of deaths caused by *Plasmodium falciparum* malaria has probably decreased in recent years, the disease remains a huge problem in much of the developing world.[1,2] Drug resistance is a major threat, and reports of resistance to artemisinins are alarming, as we are now highly dependent on the use of artemisinin-based combination therapies (ACTs) to treat *falciparum* malaria.[3−5] Semisynthetic artemisinin derivatives (Figure 1) were a major breakthrough in malaria chemotherapy because they produce a very rapid therapeutic response against malaria parasites. ACT, the current recommended treatment for uncomplicated *falciparum* malaria in most of the world, includes five standard regimens, each incorporating a rapid acting artemisinin derivative plus a slower acting drug to kill parasites that may escape the rapid action of the artemisinin and to limit selection of artemisinin-resistant parasites.[6] Artemisinins and other endoperoxides, such as tetraoxane **2** (Figure 1), are highly active against the asexual erythrocytic stage of infection. These compounds are reductively activated in the presence of high concentrations of iron(II) accumulated inside the parasite food vacuole after the digestion of large quantities of host hemoglobin. Although the mechanism of action of artemisinins is still a matter of debate,[7] it is generally accepted that the resulting radicals of this activation can alkylate several targets in the parasite, leading to its death.

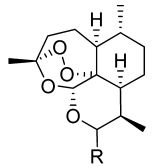

1, R = =O, ART
R = α-OH, DHA
R = β-OMe, AM
R = α-CO(CH$_2$)$_2$CO$_2$H, AS

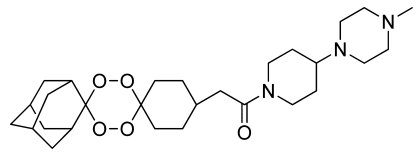

2

Figure 1. Structures of artemisinin, **1**, its derivatives dihydroartemisinin (DHA), artemether (AM), and artesunate (AS) and the tetraoxane RKA182, **2**.

A key feature of hybrid drugs is the presence of different mechanisms of action, against either a single target or different targets.[8] A recent publication associates artemisinin resistance

Received: March 22, 2014
Published: May 13, 2014

   dx.doi.org/10.1021/jm5004528 | J. Med. Chem. 2014, 57, 4916−4923

to a form of antioxidant defense system,[9] so it is particularly important that a distinct mechanisms of action is combined with endoperoxide drugs in the treatment of highly adaptable parasites.[10] We recently reported that tetraoxane−peptide vinyl sulfone hybrids, **3** (Figure 2), are rapidly activated by iron(II),

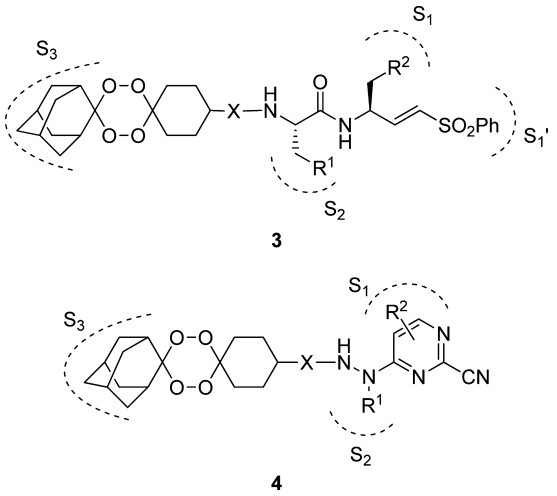

Figure 2. General structures: tetraoxane−vinyl sulfone hybrids **3**; tetraoxane−pyrimidine nitrile hybrids **4**.

releasing a potent irreversible inhibitor of falcipains inside the parasitedigestive vacuole.[11] Falcipain-2 and falcipain-3 are cysteine proteases from *P. falciparum* involved in the digestion of host hemoglobin in the digestive vacuole of the parasite, providing amino acids for its survival and development.[12] Although hybrid compounds **3** displayed weak to moderate falcipain inhibitory activity, they were able to inhibit hemoglobin digestion at low nanomolar concentrations, consistent with the release of the parent peptide vinyl sulfone triggered by iron(II).

To overcome selectivity issues often associated with irreversible inhibitors, it is desirable to develop nonpeptidic reversible inhibitors.[12,13] Nitriles inhibit cysteine proteases by forming a reversible thioimidate intermediate resulting from the nucleophilic attack of the catalytic cysteine residue.[14−18] Several heterocyclic and peptidomimetic compounds containing a nitrile warhead displayed excellent inhibitory activity against falcipain-2 and against cultured *P. falciparum*.[19] In particular, appropriately decorated pyrimidine and triazine scaffolds were shown to position vectors for the S_1, S_2, and S_3 binding pockets and to direct the thioimidate adduct toward the oxyanion hole of the enzyme.[18,19] An interesting feature of pyrimidine nitriles is the possibility to accommodate a wide variety of substituents at P_3, without significantly compromising enzyme inhibition.[19] This observation prompted us to hypothesize that tetraoxane−pyrimidine nitrile constructs with the general structure **4** (Figure 2), in which the peroxide moiety occupies the P_3 position, could be endowed with both falcipain and *P. falciparum* inhibitory activities, in contrast to their hybrid vinyl sulfone counterparts **3**.[11] This approach could provide a new class of hybrid compounds whose ability to inhibit falcipains would not be dependent on the rate of peroxide activation triggered by theiron(II) present in the digestive vacuole of the malaria parasite. We now report the synthesis of tetraoxane−pyrimidine nitrile hybrids **4**, and the evaluation of these compounds against the blood and liver stages of malaria infection, against falcipain-2, against mammalian cells, and in vivo using a murine model of malaria. The adamantane-based tetraoxane moiety was selected throughout this study, as it is known to provide adequate metabolic stability.

RESULTS AND DISCUSSION

Synthesis. Tetraoxane−pyrimidine nitrile hybrids were synthesized as depicted in Schemes 1 and 2. The tetraoxane

Scheme 1. Synthesis of Tetraoxanes 6 and 7[a]

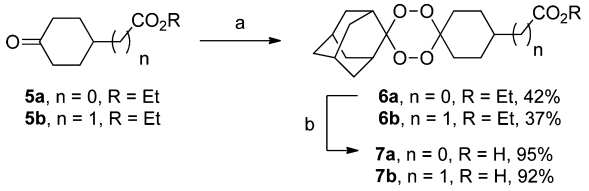

[a]Reagents and conditions: (a) (1) HCO_2H, H_2O_2 50%, ACN, rt, 45 min, (2) 2-adamantanone, Re_2O_7, DCM, rt, 3 h; (b) NaOH, MeOH/H_2O (2:1), 80 °C, 1 h 30 s.

moiety was prepared by reacting the appropriate ketone **5** with hydrogen peroxide 50% in acidic conditions to form a *gem*-dihydroperoxide intermediate, which was then reacted with 2-adamantanone in the presence of rhenium(VII) catalyst to give **6a−b** (Scheme 1).[20,21] The synthesis of the pyrimidine nitrile moiety followed the procedure reported by Coterón et al.[19] Reductive amination of *tert*-butyl carbazate, **8**, with the appropriate aldehyde or ketone and subsequent nucleophilic aromatic substitution reaction of the appropriate 2,4-dichloropyrimidine with hydrazines **9a−c** afforded the 5- and 6-substituted 2-chloropyrimidines **10a−f** (Scheme 2). Cyanation of **10a−f** using potassium cyanide gave the corresponding 2-cyanopyrimidines **11a−f**.[19] Boc removal with *p*-toluenesulfonic acid and subsequent coupling with the acid chloride derived from **7** yielded the final products **4** with poor to moderate yields (Scheme 2, method A). Alternatively, deprotection of the hydrazine **10a−f** followed by coupling with the acid chloride derived from **7** and cyanation of the 2-chloropyrimidine hybrid precursors **12** afforded the final products in moderate to good yields (Scheme 2, method B).

Iron(II) Activation. Compound **13**, lacking the tetraoxane core, was prepared from the reductive cleavage of tetraoxane **4a** using iron(II) bromide in dichloromethane (Scheme 3).[22] This reaction is intended to simulate the intraparasitic endoperoxide iron(II) mediated bioactivation process in the digestive vacuole of the parasite.[11,22] To confirm the proposed mechanism, an aqueous solution of **4a** was treated with high concentration of iron(II) sulfate, and the resulting mixture was analyzed by LC-MS.[22] Decomposition of **4a** into ketone **13** followed first-order decay kinetics, with a half-life of 5.1 h (Figure 3). This value is of the same order of magnitude as those observed with tetraoxanes and 1,2,4-trioxolane analogues with basic side chains, suggesting that the nature of the endoperoxide side chain does not significantly affect the rate of iron(II)-triggered activation.[22]

As depicted in Figure 3, ketone **13** accounts for 50% of the initial concentration of **4a**, indicating that another decomposition pathway is operating under the conditions used. Tetraoxane activation may involve coordination of iron(II) either with O2, leading to the formation of **13**, or with O1, which leads to 2-adamantanone (Supporting Information Scheme S1). Although we were not able to detect 2-

dx.doi.org/10.1021/jm5004528 | J. Med. Chem. 2014, 57, 4916−4923

Scheme 2. Synthesis of Tetraoxanes–Pyrimidine Nitrile Hybrids 4a–g[a]

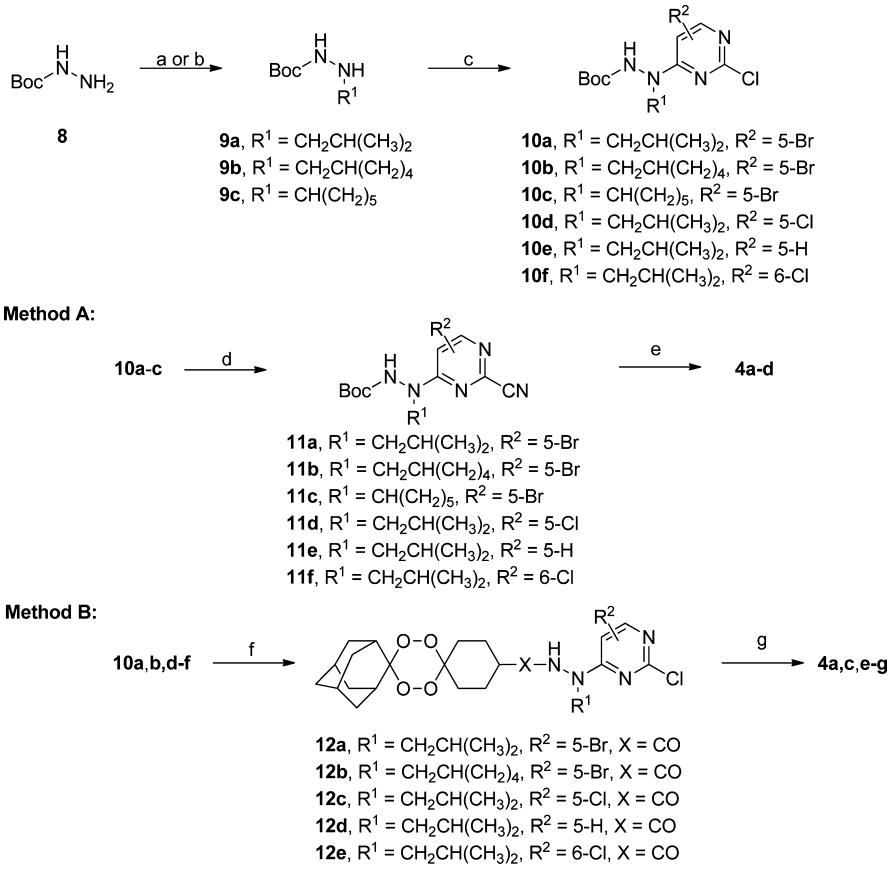

[a]Reagents and conditions: (a) (1) aldehyde, dry DCM, molecular sieves 3 Å (2) Et_3SiH, Pd/C, dry MeOH; (b) aldehyde or ketone, dry DCM, glacial AcOH, $NaBH(OAc)_3$, rt, ov; (c) 2,4-dichloropyrimidines, DIPEA, iPrOH, reflux, ov; (d) KCN, DABCO, DMSO/H_2O (9:1), rt, 3 h; (e) (1) pTsOH, ACN, rt, ov, (2) acid chloride of tetraoxane **7a–b**, DIPEA, dry THF, rt, ov; (f) (1) pTsOH, ACN, rt, ov, (2) acid chloride of tetraoxane **7a**, DIPEA, dry THF, rt, ov; (g) KCN, DABCO, DMSO/H_2O (9:1), rt, 3 h.

Scheme 3. Synthesis of Pyrimidine Nitrile 13[a]

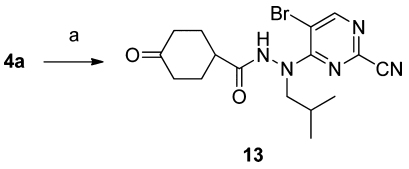

[a]Reagents and conditions: (a) $FeBr_2$, ACN/DCM (1:1), rt, 24 h.

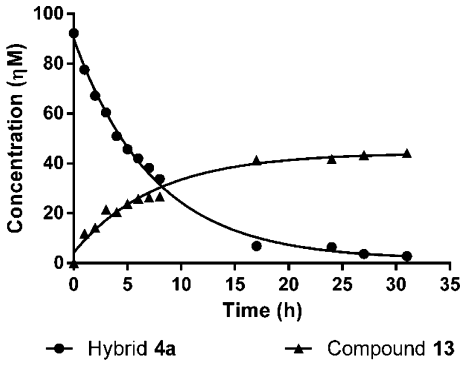

Figure 3. Time-dependence profile for the activation of hybrid **4a** by 18 equiv of $FeSO_4$ in aqueous acetonitrile.

adamantanone, these results are in agreement with similar assays, where radicals derived from both activation pathways were trapped with TEMPO and identified.[20,22]

Falcipain-2 Inhibition. Compounds **4** were screened against recombinant falcipain-2. They displayed a wide range of inhibitory activities, with IC_{50}s ranging from 978 nM for **4g** to 3.4 nM for **4e** (Table 1). These results suggest that pyrimidine nitriles, in contrast to their vinyl sulfone hybrid counterparts **3**,[11] can accommodate the bulky adamantane–tetraoxane moiety at P_3 without significantly affecting the enzyme inhibitory activity. Structure–activity data revealed that substituents at C-5 of the pyrimidine, which interact with the S_1 pocket, markedly affect the potency, with compounds bearing a chlorine and bromine 270 and 55 times more potent than their unsubstituted counterparts, respectively (**4a** and **4e** versus **4f**). In contrast, a chlorine atom at C-6 had a deleterious effect on the inhibitory capacity, compared to the unsubstituted compound (**4g** versus **4f**), suggesting that substituents at this position do not interact adequately with the S_1 binding site. Extending the linker between the two pharmacophoric moieties decreased the activity by 6-fold (**4a** versus **4b**). Finally, varying the P_2 moiety suggested that the isobutyl and cyclohexyl groups are well accommodated by the S_2 binding pocket, a result in line with that reported by Coterón et al.[19]

The predicted binding modes of hybrids **4** were further supported by covalent molecular docking calculations. The

dx.doi.org/10.1021/jm5004528 | J. Med. Chem. 2014, 57, 4916–4923

Table 1. Antiplasmodial Activity against Chloroquine-Sensitive (3D7), Chloroquine-Resistant (W2), and Atovaquone-Resistant (FCR3) Strains of *P. falciparum*, Falcipain-2 (FP-2) Inhibition, and Digestive Vacuole (DV) Swelling Induced by Hybrids 4a–g and Ketone 13

				IC_{50} (nM)				
compd	X	R^1	R^2	3D7	W2	FCR3	FP-2	DV swelling (123 nM)[a]
4a	CO	$-CH_2CH(CH_3)_2$	5-Br	58.1 ± 7.8	9.8 ± 1.5	ND[b]	16.4 ± 4.2	yes
4b	CH_2CO	$-CH_2CH(CH_3)_2$	5-Br	18.9 ± 4.2	22.8 ± 2.8	ND[b]	95.1 ± 0.4	yes
4c	CO	$-CH_2CH(CH_2)_4$	5-Br	70.7 ± 1.2	29.5 ± 11.7	ND[b]	112 ± 9	ND[b]
4d	CO	$-CH(CH_2)_5$	5-Br	78.5 ± 8.4	22.4 ± 12.3	81.2 ± 7.2	25.3 ± 7.1	yes
4e	CO	$-CH_2CH(CH_3)_2$	5-Cl	80.9 ± 17.2	33.8 ± 0	53.3 ± 7.6	3.4 ± 0.6	yes
4f	CO	$-CH_2CH(CH_3)_2$	5-H	13.1 ± 0.6	47.3 ± 1.7	30.3 ± 9.4	909 ± 93	no
4g	CO	$-CH_2CH(CH_3)_2$	6-Cl	28.4 ± 7.9	48.9 ± 2.5	37.7 ± 6.4	978 ± 205	no
13				48.2 ± 11.1	48.1 ± 3.2	ND[b]	58.4 ± 0.4	yes
ART				36.2 ± 4.7	14.1 ± 1.4	7.7 ± 8.7		
CQ				9.25 ± 3.5	64.7 ± 5.5	36.2 ± 0.4		

[a]Observation of DV swelling at 123 nM concentration. [b]ND: not determined.

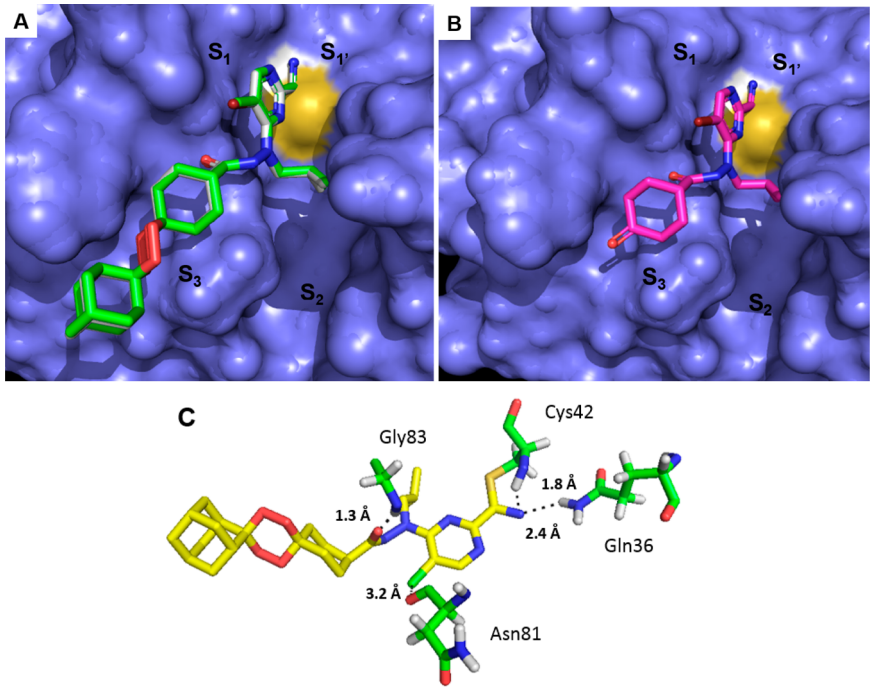

Figure 4. (A) Superimposition of docked conformations of hybrids **4a** (green) and **4e** (light-gray) inside FP-2 binding pocket. (B) Docked conformation of ketone **13** inside FP-2 binding pocket. (C) Closer view of the interactions between compound **4e** and residues present in the FP-2 binding pocket.

crystal structure of FP-2 complexed with the epoxysuccinate E64 at a resolution of 2.9 Å (PDB code: 3BPF) was employed in the docking calculations. Inspection of the top ranking solutions of **4a**, **4b**, **4e–g**, and **13** inside the falcipain-2 binding pocket (Figure 4A; see Supporting Information for a closer view), selected according to their goldscore fitness function, revealed that these compounds present the pyrimidine thioimidate adduct resulting from the nucleophilic attack of the active site cysteine sitting in the S_1 binding pocket, while the isobutyl group and tetraoxane moiety fit into the S_2 and S_3 binding sites, respectively. Remarkably, the parent ketone **13** adopts the same pose as **4a** and **4e** (Figure 4B), indicating that the adamantane group do not significantly disturb the positioning of the pyrimidine inside the active site. The best poses reveal that nitrogen atom of the thioimidate adduct is stabilized by hydrogen bonding with Gln36 (N···H ∼ 2.4 Å) and Cys42 (N···H ∼ 1.8 Å), while the carbonyl oxygen atom establishes a hydrogen bond with Gly83 (O···H ∼ 1.3 Å). But the most prominent feature observed for derivatives **4a**, **4b**, and **4e** is the strong halogen bond established between 5-Br/5-Cl and the Asn81 oxygen atom, ranging from 2.8 to 3.2 Å (Figure 4C). These values are lower than the sum of the van der Waals radii of 3.27 Å[23] and contrasts with the value of 3.54 Å observed for the less potent 6-Cl counterpart **4g**.

Target engagement in the parasites was confirmed by the observation that cultured parasites incubated with compounds **4** at 123 nM for 24 h beginning at the ring stage developed swollen digestive vacuoles with the staining characteristics of erythrocyte cytoplasm (Table 1). It has been previously shown that this specific abnormality is indicative of a block in hemoglobin hydrolysis caused by inhibition of falcipains.[24] Remarkably, compounds **4** with low nanomolar IC_{50} values against falcipain-2 were able to block hemoglobin degradation

dx.doi.org/10.1021/jm5004528 | J. Med. Chem. 2014, 57, 4916–4923

at 123 nM to the same extent as the parent pyrimidine nitrile **13**.

In Vitro Antimalarial Activity. Hybrid compounds **4** were screened against chloroquine-sensitive (3D7), chloroquine-resistant (W2), and atovaquone-resistant (FCR-3) *P. falciparum* strains to assess their potential as blood stage antimalarials (Table 2). Compounds **4a−g** inhibited the growth of the three

Table 2. In Vitro Cytotoxicity and Selectivity Index of Hybrids 4a−g and Ketone 13

	CC_{50} (μM)		selectivity index (SI)[a]	
compd	Hek293T	NIH3T	Hek293T	NIH3T
4a	>100	8.0 ± 0.7	>10000	816
4b	85.5 ± 6.7	2.3 ± 1.0	3750	101
4c	>100	5.5 ± 0.5	>3390	186
4d	>100	1.4 ± 0.1	>4464	63
4e	>100	4.5 ± 1.3	>2959	133
4f	>100	0.9 ± 0.1	>2114	19
4g	>100	1.7 ± 0.8	>2045	35
13	>100	>100	>2079	>2079

[a]SI was calculated as the ratio of IC_{50} for in vitro cytotoxicity on Hek293T and NIH3T to the IC_{50} of plasmodial inhibition against the strain W2.

P. falciparum strains with IC_{50} values ranging from 9.8 to 81.2 nM, while displaying negligible cytotoxicity, with EC_{50} values against HEK293T mammalian cells ranging from 85 to >100 μM.

Activity against liver-stage malaria parasites is highly desirable, in particular for radical cure of *Plasmodium vivax* and *Plasmodium ovale* infections and in drugs used for the prevention of malaria.[25,26] Thus, compounds **4** were also evaluated for their activity against liver stages of the rodent parasite *Plasmodium berghei* and for cytotoxicity to Huh-7 human hepatoma cells, employing previously reported methods.[27] Primaquine, the only approved drug to treat liver stage/relapsing malaria, and atovaquone were also included as positive controls for liver stage activity. Most hybrid compounds **4** significantly decreased the parasite load in Huh-7 cells when compared to untreated controls and were more active than primaquine at 10 μM (Figure 5) but less active than atovaquone at 2 μM (see Figure S3 in Supporting Information). A similar activity profile was observed for the parent compound **13**. The endoperoxide artemisinin was inactive at both dose levels. To our knowledge, this is the first report of endoperoxides and pyrimidine nitriles active against liver stage malaria. So far, only hybrid compounds based on known liver stage antimalarials[27−29] were noted to have both blood and liver stage activity.

In Vivo Efficacy. Hybrid **4e** was selected to evaluate the in vivo efficacy in a murine model of infection as it displayed excellent FP-2 inhibitory activity, high potency against all *P. falciparum* strains, low cytotoxicity, and very good activity in the liver stage assay. Hybrid **4e** was tested at 30 mg/kg/day, administered intraperitoneally for five consecutive days beginning when parasitemia reached 4% at day 4 postinfection. Infected mice receiving compound **4e** responded initially to the treatment, but parasitemia increased after day 8, to reach a mean valueof 51% at day 18 postinfection. However, all animals treated with compound **4e** survived to day 18 after initial inoculation with parasites (Figure 6).

CONCLUSIONS

In conclusion, we developed a series of tetraoxane−pyrimidine nitrile hybrids **4** endowed with two distinct mechanisms of action, a feature predicted to help prevent selection of drug resistance. Remarkably, appending a large adamantane-based tetraoxane moiety to the P_3 position of the pyrimidine scaffold did not affect inhibitory potency against falcipain-2 or general structure−activity relationship trends when compared to previously reported pyrimidine nitriles. Although this enzyme inhibitory profile translated into excellent in vitro potency against the erythrocytic stage malaria parasites, there was only moderate in vivo efficacy. Overall, this new class of hybrid antimalarial compounds displayed good activity against the blood and liver stages of malaria parasites and it is thus deserving of further exploration.[26]

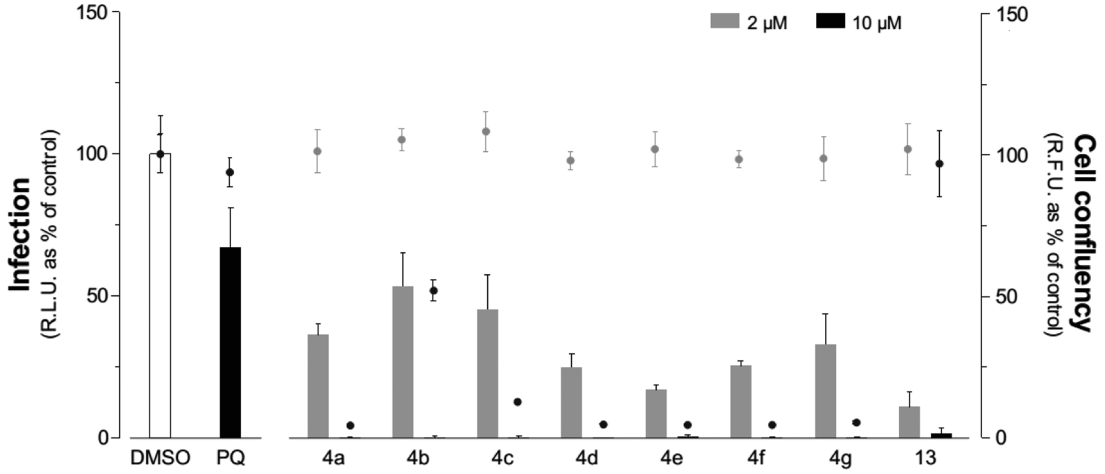

Figure 5. In vitro antimalarial activity against the liver stage of infection. In vitro inhibition of hepatic *P. berghei* infection by compounds **4a−g** and **13**. Compounds were added to Huh-7 hepatoma cells 1 h before infection with luciferase-expressing sporozoites. An amount of DMSO equivalent to that in the highest compound concentration tested was used as a control. Then 48 h after the addition of *P. berghei* sporozoites, cell confluence (dots on bar plots) was assessed by AlamarBlue fluorescence, and the infection rate (bars) was measured by quantifying the luciferase activity by luminescence. The effects of two concentrations (2 and 10 μM) of compounds **4a−g** and **13** are shown. Results are expressed as means ± standard deviations.

dx.doi.org/10.1021/jm5004528 | J. Med. Chem. 2014, 57, 4916−4923

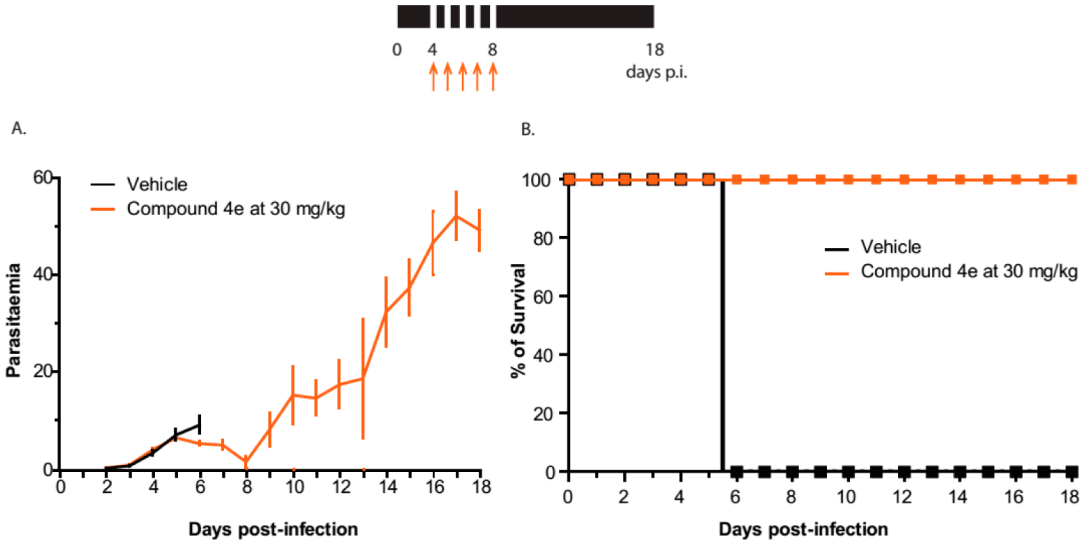

Figure 6. In vivo mouse efficacy studies for compound **4e** in the *P. berghei* mouse model. Mice were infected with parasites on day 0, and compound **4e** dosing began on day 4 and lasted for a total of 5 consecutive days (indicated by the arrows). Dosing was by ip administration at 30 mg/kg bw. (A) Parasitemia curve; (B) survival curve.

EXPERIMENTAL SECTION

Chemistry. All chemicals and solvents were of analytical reagent grade and were purchased from Alfa Aesar or Sigma-Aldrich. Tetrahydrofuran was dried before use. Thin layer chromatography was performed using Merck silica gel 60F254 aluminum plates and visualized by UV light, iodine, potassium permanganate dip, and/or *p*-anisaldehyde dip. Flash column chromatography was performed using Merck silica gel 60 (230−400 mesh ASTM) eluting with various solvent mixtures and using an air aquarium pump to apply pressure. NMR spectra were recorded on a Bruker 400 Ultra-Shield (400 MHz) in $CDCl_3$; chemical shifts, δ, are expressed in ppm, and coupling constants, J, are expressed in Hz. Mass analyses were determined using a Micromass Quattro Micro API spectrometer, equipped with a Waters 2695 HPLC module and Waters 2996 photodiode array detector. High resolution mass spectra were performed in Unidade de Espectrometria de Masas (HMRS-ESI-TOF), Santiago de Compostela, Spain. All compounds tested in the biological assays were determined to be >95% pure by elemental analysis (for C, H, and N). Melting points were determined using a Kofler Bock Monoscop M and are uncorrected.

Preparation of Compounds ***4*** *(Method A).* (1) To a solution of compound **11a−f** (0.2 mmol) in ACN (1.5 mL) was added *p*-toluenesulfonic acid (0.8 mmol). The mixture was stirred overnight at room temperature. Then the solvent was removed under reduced pressure and the crude taken up in EtOAc (30 mL) and washed with 1 M solution of Na_2CO_3 (30 mL). The aqueous phase was further extracted with EtOAc (2 × 20 mL). The combined organic phases were dried over Na_2SO_4, filtered, and concentrated to give the free amine. (2) A solution of tetraoxane **7a−b** (0.24 mmol) in thionyl chloride (2 mL) was refluxed for 2 h. The mixture was concentrated under reduced pressure, and then the acid chloride was taken up in dry THF (1 mL) in nitrogen atmosphere. A solution of the appropriate free amine (0.2 mmol) in dry THF (1 mL) was added to the acid chloride. After stirring for 30 min at room temperature under nitrogen, DIPEA (0.6 mmol) was added, followed by overnight stirring in the same conditions. The mixture was diluted with DCM (30 mL) and water (30 mL), and the phases were separated. The aqueous phase was further extracted with DCM (2 × 20 mL). The combined organic extracts were dried over Na_2SO_4, filtered, and concentrated. Purification by flash chromatography gave the pure compound.

Preparation of Compounds ***4*** *(Method B).* To a solution of compound **12a−e** (0.2 mmol) and DABCO (0.2 mmol) in DMSO/water (9:1, 2 mL) was added KCN (0.22 mmol). The solution was stirred for 5 h at room temperature. Then the mixture was poured into ice water (30 mL) and extracted with EtOAc (2 × 30 mL). The combined organic phases were washed with saturated solution of $NaHCO_3$ (30 mL), dried over Na_2SO_4, filtered, and concentrated. Purification by flash chromatography gave the pure compound.

Compound ***4a.*** White solid (method A: 38% yield/method B: 60% yield); mp 113−114 °C. ^{1}H NMR (400 MHz, $CDCl_3$) δ = 8.47 (s, 1H), 7.79 (s, 1H), 3.67 (bs, 2H), 2.38 (bs, 1H), 2.11−1.46 (m, 23H), 0.99 (d, J = 6.5 Hz, 6H) ppm. ^{13}C NMR (101 MHz, $CDCl_3$) δ = 171.9, 160.7, 160.7, 141.6, 115.4, 110.7, 106.7, 106.2, 59.0, 41.6, 36.9, 33.1, 27.0, 26.3, 20.2 ppm. HRMS-ESI: m/z $[M + Na]^+$ calcd for $C_{26}H_{34}BrN_5O_5$, 598.1641; found, 598.1618.

Compound ***4b.*** White solid (method A: 27% yield); mp 94−96 °C. ^{1}H NMR (400 MHz, $CDCl_3$) δ = 8.46 (s, 1H), 7.63 (s, 1H), 3.67 (bs, 2H), 2.19 (d, J = 6.7 Hz, 2H), 2.09−1.46 (m, 22H), 1.41−1.20 (m, 2H), 0.96 (d, J = 6.7 Hz, 6H) ppm. ^{13}C NMR (101 MHz, $CDCl_3$) δ = 169.6, 160.7, 160.6, 141.6, 115.4, 110.6, 107.5, 106.0, 59.1, 39.5, 36.9, 33.3, 33.1, 33.1, 27.0, 27.0, 26.3, 20.2 ppm. HRMS-ESI: m/z $[M + H]^+$ calcd for $C_{27}H_{37}BrN_5O_5$, 590.1978; found, 590.1961.

Compound ***4c.*** White solid (method A: 10% yield/method B: 66% yield); mp 190−191 °C. ^{1}H NMR (400 MHz, $CDCl_3$) δ = 8.44 (s, 1H), 7.69 (s, 1H), 3.75 (bs, 2H), 2.42−2.31 (m, 1H), 2.25−2.15 (m, 1H), 2.07−1.47 (m, 26H), 1.27 (m, 4H) ppm. ^{13}C NMR (101 MHz, $CDCl_3$) δ = 172.0, 160.7, 160.7, 141.8, 115.5, 110.9, 106.8, 106.2, 56.4, 41.7, 37.5, 37.0, 33.2, 30.7, 27.1, 27.1, 25.2 ppm. HRMS-ESI: m/z $[M + H]^+$ calcd for $C_{28}H_{37}BrN_5O_5$, 602.1978; found, 602.1962.

Compound ***4d.*** White solid (method A: 8% yield); mp 148−149 °C. ^{1}H NMR (400 MHz, $CDCl_3$) δ = 8.41 (s, 1H), 7.47 (s, 1H), 4.54 (bs, 1H), 2.42 (bs, 1H), 2.13−1.20 (m, 31H), 1.20−1.01 (m, 2H) ppm. ^{13}C NMR (101 MHz, $CDCl_3$) δ = 172.5, 160.4, 159.6, 141.7, 115.5, 110.7, 106.7, 106.3, 59.6, 36.9, 33.1, 27.0, 25.5 ppm. HRMS-ESI: m/z $[M + H]^+$ calcd for $C_{28}H_{37}BrN_5O_5$, 602.1978; found, 602.1971.

Compound ***4e.*** White solid (method B: 57% yield); mp 134−137 °C. ^{1}H NMR (400 MHz, $CDCl_3$) δ = 8.28 (s, 1H), 7.79 (s, 1H), 3.66 (bs, 2H), 2.40−2.27 (m, 1H), 2.08−1.46 (m, 23H), 0.97 (d, J = 6.7 Hz, 6H) ppm. ^{13}C NMR (101 MHz, $CDCl_3$) δ = 172.2, 159.8, 157.7, 141.1, 117.7, 115.3, 110.7, 106.7, 59.2, 41.6, 36.9, 33.1, 27.0, 27.0, 26.4, 20.2 ppm. HRMS-ESI: m/z $[M + H]^+$ calcd for $C_{26}H_{35}ClN_5O_5$, 532.2327; found, 532.2312.

Compound ***4f.*** White solid (method B: 43% yield); mp 196−197 °C. ^{1}H NMR (400 MHz, $CDCl_3$) δ = 8.22 (d, J = 6.0 Hz, 1H), 8.06 (bs, 1H), 6.61 (d, J = 6.0 Hz, 1H), 3.97−3.25 (m, 2H), 2.47−2.33 (m, 1H), 2.07−1.47 (m, 23H), 0.93 (d, J = 6.5 Hz, 6H) ppm. ^{13}C NMR (101 MHz, $CDCl_3$) δ = 158.5, 156.2, 144.1, 116.0, 110.7, 106.7, 105.6,

dx.doi.org/10.1021/jm5004528 | *J. Med. Chem.* 2014, 57, 4916−4923

41.8, 36.9, 33.1, 29.7, 27.0, 26.7, 20.1 ppm. HRMS-ESI: m/z [M − H]$^-$ calcd for $C_{26}H_{34}N_5O_5$, 496.2560; found, 496.2568.

Compound ***4g***. White solid (method **B**: 37% yield); mp 106−108 °C. ^{1}H NMR (400 MHz, $CDCl_3$) δ = 7.58 (s, 1H), 6.60 (s, 1H), 3.98−3.13 (m, 2H), 2.40 (bs, 1H), 2.14−1.46 (m, 23H), 0.95 (d, J = 6.4 Hz, 6H) ppm. ^{13}C NMR (101 MHz, $CDCl_3$) δ = 160.7, 143.5, 115.0, 110.8, 106.6, 104.6, 41.9, 36.9, 33.1, 27.0, 26.7, 20.1 ppm. HRMS-ESI: m/z [M − H]$^-$ calcd for $C_{26}H_{33}ClN_5O_5$, 530.2170; found, 530.2173.

In Vitro Activity Assay against Blood Stage of Infection. Synchronized ring-stage *P. falciparum* strain W2 parasites were cultured with multiple concentrations of test compounds (added from 1000× stocks in DMSO) in RPMI 1640 medium with 10% human serum. After 48 h of incubation, when control cultures contained new rings, parasites were fixed with 1% formaldehyde in phosphate-buffered saline (PBS), pH 7.4, for 48 h at room temperature; then they were labeled with YOYO-1 (1 nM; Molecular Probes) in 0.1% Triton X-100 in PBS. Parasitemia was determined from dot plots (forward scatter versus fluorescence) acquired on a FACSort flow cytometer using CellQuest software (Becton Dickinson). Fifty percent inhibitory concentrations (IC_{50} values) for growth inhibition were determined with GraphPad Prism software from plots of the percentage of parasitemia of the control relative to the inhibitor concentration. In each case, the goodness of the curve fit was documented by R^2 values of 0.95.

In Vitro Activity against Liver Stage of Infection. Inhibition of liver-stage infection by test compounds was determined by measuring the luminescence intensity in Huh-7 cells infected with a firefly luciferase expressing *P. berghei* line, PbGFP-Luc_{con}, as previously described.[30] Huh-7 cells, from a human hepatoma cell line, were cultured in 1640 rpmI medium supplemented with 10% v/v fetal calf serum, 1% v/v nonessential amino acids, 1% v/v penicillin/streptomycin, 1% v/v glutamine, and 10 mM 4-(2-hydroxyethyl)-1-piperazineethanesulfonic acid (HEPES), pH 7, and maintained at 37 °C with 5% CO_2. For infection assays, Huh-7 cells (1.2×10^4 per well) were seeded in 96-well plates the day before drug treatment and infection. The medium was replaced by medium containing the appropriate concentration of each compound approximately 1 h prior to infection with sporozoites freshly obtained through disruption of salivary glands of infected female *Anopheles stephensi* mosquitoes. Sporozoite addition was followed by centrifugation at 1700*g* for 5 min. Then 24 h after infection, the medium was replaced by fresh medium containing the appropriate concentration of each compound. Parasite infection load was measured 48 h after infection. The effect of the compounds on the viability of Huh-7 cells was assessed by the AlamarBlue assay (Invitrogen, U.K.) using the manufacturer's protocol.

Falcipain-2 Inhibition Assay. IC_{50}s against falcipain-2 were determined as described earlier.[24] Briefly, equal amounts (∼1 nM) of recombinant falcipain-2 were incubated with different concentrations of vinyl sulfones (added from 100× stocks in DMSO) in 100 mM sodium acetate (pH 5.5)−10 mM dithiothreitol for 30 min at room temperature before addition of the substrate benzoxycarbonyl-Leu-Arg-7-amino-4-methyl-coumarin (final concentration, 25 μM). Fluorescence was continuously monitored for 30 min at room temperature in a Labsystems Fluoroskan II spectrofluorometer. IC_{50}s were determined from plots of activity over enzyme concentration with GraphPad Prism software.

In Vivo Assay. C57Bl/6J mice were infected by intraperitoneal inoculations of 2×10^6 GFP-expressing *P. berghei* ANKA-infected erythrocytes. Parasitemias were monitored daily by microscopy and flow cytometry. Drug treatment was initiated when blood parasitemias were ca. 3.9%. At this point, 30 mg/kg bw of compound **4a** were administered once daily by intraperitoneal injection for 5 days. An equivalent amount of drug vehicle was injected in control mice. Parasitemias, disease symptoms, and survival were monitored daily from the onset of treatment until the end of the experiment. The experiment was terminated following 10 consecutive of growing blood parasitemia in treated mice. Parasitemias of control mice increased steadily until day 6 postinfection, when all mice died with symptoms of experimental cerebral malaria.

■ ASSOCIATED CONTENT

Ⓢ Supporting Information

Experimental details for the preparation of compounds **7a−b** and **11−13**, the description of iron(II) activation of hybrid **4a**, and computational methodology. This material is available free of charge via the Internet at http://pubs.acs.org.

■ AUTHOR INFORMATION

Corresponding Authors

*For P.M.O.: phone, 0151-794-3553; E-mail, p.m.oneill01@liverpool.ac.uk.

*For R.M.: fax, + 351 217946470; E-mail, rmoreira@ff.ul.pt.

Author Contributions

The manuscript was written through contributions of all authors. All authors have given approval to the final version of the manuscript.

Notes

The authors declare no competing financial interest.

■ ACKNOWLEDGMENTS

This work was supported by Fundação para a Ciência e Tecnologia, Portugal: grants PTDC/SAU-FAR/118459/2010, PEst-OE/SAU/UI4013/2014, REDE/1501/REM/2005, and PTDC/SAU-MIC/117060/2010; fellowship SFRH/BD/63200/2009 to R.O.), and FundaçãoLuso−Americana (award to R.M.).

■ ABBREVIATIONS USED

ACT, artemisinin-based combination therapy; ART, artemisinin; CQ, chloroquine; FP-2, falcipain-2

■ REFERENCES

(1) *World Malaria Report 2013*; World Health Organization: Geneva, 2013.

(2) White, N. J.; Pukrittayakamee, S.; Hien, T. T.; Faiz, M. A.; Mokuolu, O. A.; Dondorp, A. M. Malaria. *Lancet* **2014**, *383*, 723−735.

(3) White, N. J. Artemisinin Resistance—The Clock Is Ticking. *Lancet* **2010**, *376*, 2051−2052.

(4) Yeung, S.; Socheat, D.; Moorthy, V. S.; Mills, A. J. Artemisinin Resistance on the Thai−Cambodian Border. *Lancet* **2009**, *374*, 1418−1419.

(5) Dondorp, A. M.; Nosten, F.; Yi, P.; Das, D.; Phyo, A. P.; Tarning, J.; Lwin, K. M.; Ariey, F.; Hanpithakpong, W.; Lee, S. J.; Ringwald, P.; Silamut, K.; Imwong, M.; Chotivanich, K.; Lim, P.; Herdman, T.; An, S. S.; Yeung, S.; Singhasivanon, P.; Day, N. P. J.; Lindegardh, N.; Socheat, D.; White, N. J. Artemisinin Resistance in *Plasmodium falciparum* Malaria. *N. Engl. J. Med.* **2009**, *361*, 455−467.

(6) *Guidelines for the Treatment of Malaria*, 2nd ed.; World Health Organization: Geneva, 2010.

(7) O'Neill, P. M.; Barton, V. E.; Ward, S. A. The Molecular Mechanism of Action of Artemisinin—The Debate Continues. *Molecules* **2010**, *15*, 1705−1721.

(8) Meunier, B. Hybrid Molecules with a Dual Mode of Action: Dream or Reality? *Acc. Chem. Res.* **2008**, *41*, 69−77.

(9) Ariey, F.; Witkowski, B.; Amaratunga, C.; Beghain, J.; Langlois, A.-C.; Khim, N.; Kim, S.; Duru, V.; Bouchier, C.; Ma, L.; Lim, P.; Leang, R.; Duong, S.; Sreng, S.; Suon, S.; Chuor, C. M.; Bout, D. M.; Ménard, S.; Rogers, W. O.; Genton, B.; Fandeur, T.; Miotto, O.; Ringwald, P.; Le Bras, J.; Berry, A.; Barale, J.-C.; Fairhurst, R. M.; Benoit-Vical, F.; Mercereau-Puijalon, O.; Ménard, D. A Molecular Marker of Artemisinin-Resistant *Plasmodium falciparum* Malaria. *Nature* **2014**, *505*, 50−55.

(10) Martinelli, A.; Moreira, R.; Ravo, P. V. L Malaria Combination Therapies: Advantages and Shortcomings. *Mini-Rev. Med. Chem.* **2008**, *8*, 201−212.
(11) Oliveira, R.; Newton, A. S.; Guedes, R. C.; Miranda, D.; Amewu, R. K.; Srivastava, A.; Gut, J.; Rosenthal, P. J.; O'Neill, P. M.; Ward, S. A.; Lopes, F.; Moreira, R. An Endoperoxide-Based Hybrid Approach to Deliver Falcipain Inhibitors Inside Malaria Parasites. *ChemMedChem* **2013**, *8*, 1528−1536.
(12) Rosenthal, P. J.; Sijwali, P. S.; Singh, A.; Shenai, B. R. Cysteine Proteases of Malaria Parasites: Targets for Chemotherapy. *Curr. Pharm. Des.* **2002**, *8*, 1659−1672.
(13) Ettari, R.; Bova, F.; Zappala, M.; Grasso, S.; Micale, N. Falcipain-2 Inhibitors. *Med. Res. Rev.* **2010**, *30*, 136−167.
(14) Greenspan, P. D.; Clark, K. L.; Cowen, S. D.; McQuire, L. W.; Tommasi, R. A.; Farley, D. L.; Quadros, E.; Coppa, D. E.; Du, Z. M.; Fang, Z.; Zhou, H. H.; Doughty, J.; Toscano, K. T.; Wigg, A. M.; Zhou, S. Y. *N*-Arylaminonitriles as Bioavailable Peptidomimetic Inhibitors of Cathepsin B. *Bioorg. Med. Chem. Lett.* **2003**, *13*, 4121−4124.
(15) Altmann, E.; Cowan-Jacob, S. W.; Missbach, M. Novel Purine Nitrile Derived Inhibitors of the Cysteine Protease Cathepsin K. *J. Med. Chem.* **2004**, *47*, 5833−5836.
(16) Ehmke, V.; Heindl, C.; Rottmann, M.; Freymond, C.; Schweizer, W. B.; Brun, R.; Stich, A.; Schirmeister, T.; Diederich, F. Potent and Selective Inhibition of Cysteine Proteases from *Plasmodium falciparum* and *Trypanosoma brucei*. *ChemMedChem* **2011**, *6*, 273−278.
(17) Ehmke, V.; Kilchmann, F.; Heindl, C.; Cui, K.; Huang, J.; Schirmeister, T.; Diederich, F. Peptidomimetic Nitriles as Selective Inhibitors for the Malarial Cysteine Protease Falcipain-2. *MedChemComm* **2011**, *2*, 800−804.
(18) Ehmke, V.; Quinsaat, J. E. Q.; Rivera-Fuentes, P.; Heindl, C.; Freymond, C.; Rottmann, M.; Brun, R.; Schirmeister, T.; Diederich, F. Tuning and Predicting Biological Affinity: Aryl Nitriles as Cysteine Protease Inhibitors. *Org. Biomol. Chem.* **2012**, *10*, 5764−5768.
(19) Coterón, J. M.; Catterick, D.; Castro, J.; Chaparro, M. J.; Díaz, B.; Fernández, E.; Ferrer, S.; Gamo, F. J.; Gordo, M.; Gut, J.; de Las Heras, L.; Legac, J.; Marco, M.; Miguel, J.; Muñoz, V.; Porras, E.; de La Rosa, J. C.; Ruiz, J. R.; Sandoval, E.; Ventosa, P.; Rosenthal, P. J.; Fiandor, J. M. Falcipain Inhibitors: Optimization Studies of the 2-Pyrimidinecarbonitrile Lead Series. *J. Med. Chem.* **2010**, *53*, 6129−6152.
(20) O'Neill, P. M.; Amewu, R. K.; Nixon, G. L.; Bousejra-El Garah, F.; Mungthin, M.; Chadwick, J.; Shone, A. E.; Vivas, L.; Lander, H.; Barton, V.; Muangnoicharoen, S.; Bray, P. G.; Davies, J.; Park, B. K.; Wittlin, S.; Brun, R.; Preschel, M.; Zhang, K.; Ward, S. A. Identification of a 1,2,4,5-Tetraoxane Antimalarial Drug-Development Candidate (RKA 182) with Superior Properties to the Semisynthetic Artemisinins. *Angew. Chem., Int. Ed. Engl.* **2010**, *49*, 5693−5697.
(21) Ghorai, P.; Dussault, P. H. Broadly Applicable Synthesis of 1,2,4,5-Tetraoxanes. *Org. Lett.* **2009**, *11*, 213−216.
(22) Bousejra-El Garah, F.; Wong, M. H.-L.; Amewu, R. K.; Muangnoicharoen, S.; Maggs, J. L.; Stigliani, J.-L.; Park, B. K.; Chadwick, J.; Ward, S. A.; O'Neill, P. M. Comparison of the Reactivity of Antimalarial 1,2,4,5-Tetraoxanes with 1,2,4-Trioxolanes in the Presence of Ferrous Iron Salts, Heme, and Ferrous Iron Salts/phosphatidylcholine. *J. Med. Chem.* **2011**, *54*, 6443−6455.
(23) Sirimulla, S.; Bailey, J. B.; Vegesna, R.; Narayan, M. Halogen Interactions in Protein−Ligand Complexes: Implications of Halogen Bonding for Rational Drug Design. *J. Chem. Inf. Model.* **2013**, *53*, 2781−2791.
(24) Rosenthal, P. J.; Olson, J. E.; Lee, G. K.; Palmer, J. T.; Klaus, J. L.; Rasnick, D. Antimalarial Effects of Vinyl Sulfone Cysteine Proteinase Inhibitors. *Antimicrob. Agents Chemother.* **1996**, *40*, 1600−1603.
(25) Derbyshire, E. R.; Mota, M. M.; Clardy, J. The Next Opportunity in Anti-Malaria Drug Discovery: The Liver Stage. *PLoS Pathog.* **2011**, *7*, e1002178.
(26) malERA Consultative Group on Drugs. A Research Agenda for Malaria Eradication: Drugs. *PLoS Med.* **2011**, *8*, e1000402.
(27) Miranda, D.; Capela, R.; Albuquerque, I. S.; Meireles, P.; Paiva, I.; Nogueira, F.; Amewu, R.; Gut, J.; Rosenthal, P. J.; Oliveira, R.; Mota, M. M.; Moreira, R.; Marti, F.; Prudêncio, M.; O'Neill, P. M.; Lopes, F. Novel Endoperoxide-Based Transmission-Blocking Antimalarials with Liver- and Blood-Schizontocidal Activities. *ACS Med. Chem. Lett.* **2013**, *5*, 108−112.
(28) Capela, R.; Cabal, G. G.; Rosenthal, P. J.; Gut, J.; Mota, M. M.; Moreira, R.; Lopes, F.; Prudêncio, M. Design and Evaluation of Primaquine−Artemisinin Hybrids as a Multistage Antimalarial Strategy. *Antimicrob. Agents Chemother.* **2011**, *55*, 4698−4706.
(29) Lödige, M.; Lewis, M. D.; Paulsen, E. S.; Esch, H. L.; Pradel, G.; Lehmann, L.; Brun, R.; Bringmann, G.; Mueller, A.-K. A Primaquine−Chloroquine Hybrid with Dual Activity against *Plasmodium* Liver and Blood Stages. *Int. J. Med. Microbiol.* **2013**, *303*, 539−547.
(30) Ploemen, I. H. J.; Prudêncio, M.; Douradinha, B. G.; Ramesar, J.; Fonager, J.; van Gemert, G. J.; Luty, A. J. F.; Hermsen, C. C.; Sauerwein, R. W.; Baptista, F. G.; Mota, M. M.; Waters, A. P.; Que, I.; Lowik, C.; Khan, S. M.; Janse, C. J.; Franke-Fayard, B. M. D. Visualisation and Quantitative Analysis of the Rodent Malaria Liver Stage by Real Time Imaging. *PLoS One* **2009**, *4*, e7881.